

Polyelectrolyte solution under spatial and dielectric confinement

Debarshee Bagchi,^{*} Trung Dac Nguyen,[†] and Monica Olvera de la Cruz[‡]
Department of Materials Science and Engineering, Northwestern University, Evanston, IL 60208
(Dated: March 22, 2021)

Polyelectrolytes under confinement are crucial for energy storage and for understanding biomolecular functions. Using molecular dynamics simulations, we analyze a polyelectrolyte solution confined between two oppositely charged planar dielectric surfaces and include surface polarization effects due to dielectric mismatch at the two electrodes. Although the effect of polarization on the charge distribution seems minor, we find that surface polarization enhances energy storage and also leads to the emergence of negative differential capacitance in confined polyelectrolyte solutions.

Polyelectrolytes exhibit a plethora of physical properties [1–4] of great interest in physical and life science, and technology. Proteins and nucleic acids are heterogeneous polyelectrolytes critical to biological function and biotechnology [5–7] while synthetic polyelectrolytes are components of modern technologies [8–11]. Various functions of polyelectrolytes in biological settings and in technological applications take place in confinement. Supercapacitors, also referred to as electrical double-layer capacitors, for example, have attracted attention because of their long life cycle, fast charging and discharging, good charge density as well as power density, reliable performance over a large temperature range, and low maintenance requirements. In a supercapacitor, usually ionic liquids or aqueous electrolyte solutions are confined between two carbon-based electrodes like graphene [12, 13]. In confinement, both simple and molecular electrolytes display intriguing phenomena, such as charge inversion and overcharging [14], breakdown of local charge neutrality [15], enhanced repulsions [16] or attractions [17], enhanced mobility [18, 19], and non-monotonic electrophoretic mobility [20].

Electrolytes and polyelectrolytes in contact with one or two oppositely charged surfaces have been extensively studied [3, 15, 16, 18, 21–28]. In reality, the dielectric constant of the charged surfaces can be very different from that of the electrolyte or the polyelectrolyte. However, the dielectric discontinuities at the electrodes require taking into account the effects of surface polarization, which is a computationally non-trivial task [22, 24, 27]. For this reason, most studies do not include surface polarization or chose to simplify the model by taking into account only one dielectric discontinuity [18, 28]. Here, along with the geometrical confinement due to the two charged impenetrable surfaces, we study the effect of dielectric confinement on a model polyelectrolyte system. We consider a salt-free aqueous polyelectrolyte solution confined between two oppositely charged planar electrodes with explicit counterions in an implicit solvent. The adsorption of the polyelectrolyte is investigated here in terms of properties of the charge accumulations near the two electrodes, commonly referred to as the *electric double-layers*.

We find that, unlike equivalent bulk polyelectrolytes with monovalent counterions or in symmetrical confined molecular electrolytes, confined polyelectrolyte solutions exhibit features such as charge amplification and charge inversion. Moreover, the energy storage in the double-layer for a con-

finned polyelectrolyte solution is found to be larger than that of a monovalent symmetric electrolyte solution under confinement. Furthermore, in presence of surface polarization effects, the energy stored is enhanced, which has possible technological implications. A crucial quantity to characterize double-layer properties is the differential capacitance that relates the change in charge storage to a small change in the voltage across the double-layer. We show that, keeping every other parameter the same, when the effects of surface polarization are included one obtains a negative differential capacitance for the double-layer formed by the polyelectrolyte molecules. Thus, although surface polarizability effects on polyelectrolyte adsorption seem to be small as has also been seen in some recent works [26, 28, 29], they play an important role in the energy storage and differential capacitance of a confined polyelectrolyte solution.

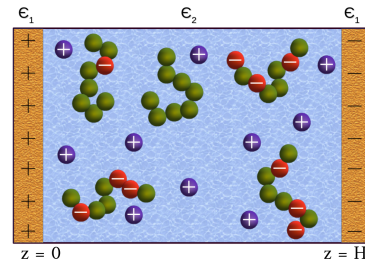


Figure 1. Schematic diagram of the polyelectrolyte model confined between two dielectric electrodes.

A schematic representation of the model system is depicted in Fig. 1. In the course grained molecular dynamics (CGMD) simulations, the polyelectrolyte is represented by a linear bead-spring chain with randomly distributed charged beads [30]. The number of charged beads on the polyelectrolyte chains is controlled by the charge fraction $f_q = n/N$, where n is the total number of charged monomer beads, each with one electron charge $-e$, and N is the total number of monomers. For overall electroneutrality we have n positive counterion beads with $+e$ charge. The simulation box dimensions are $L_x = L_y = L = 30\sigma$ and $Lz = H = 100\sigma$, where our length unit σ is the diameter of all the beads used in the simulation (we set $\sigma = 1$ which corresponds to $\sigma = 0.3$ nm in real units). The two planar electrodes are also composed of beads and are oppositely charged. Each electrode has a

charge density Σ and are located at $z = 0$ (positive electrode) and $z = H$ (negative electrode). The electrodes are considered to be composed of a material of low dielectric constant $\epsilon_1 = 2$. The solvent is a continuum background with uniform dielectric constant $\epsilon_2 = 80$ and is a poor solvent for the partially charged polyelectrolyte chains. The $N_m = 40$ monomers on each of the $N_c = 60$ polyelectrolyte chains interact via a truncated-shifted Lennard Jones (LJ) potential $V_{ij}^{LJ}(r) = 4\epsilon [(\sigma/r)^{12} - (\sigma/r)^6]$, where $\epsilon = k_B T$ is the energy scale which we set to unity in reduced units, cutoff $r_c = 2.5\sigma$ such that $V_{LJ}(r > r_c) = 0$, and T is the temperature. All other short-range interactions are purely repulsive LJ potential (Weeks-Chandler-Andersen) with $r_c = 2^{1/6}\sigma$. Two charged beads interact with each other via the long-range Coulomb potential $V_{ij}^q(r) = k_B T l_B \frac{q_i q_j}{r}$, where q_i, q_j are the valencies of the charged beads and l_B is the Bjerrum length $l_B = \frac{e^2}{\epsilon_0 \epsilon_r k_B T}$ (all the symbols have their usual meaning); we set $l_B = 0.7$ nm for water. Coulomb interactions among charged monomers and counterions are computed using $\epsilon_r = \epsilon_2$ and with the surface beads using $\epsilon_r = \frac{1}{2}(\epsilon_1 + \epsilon_2)$ [31] (see Fig. 1), and are computed using the particle-particle particle-mesh (PPPM) method with an accuracy of 10^{-4} and slab corrections [32]. The consecutive beads in the polyelectrolyte chain are connected by finite extensible nonlinear elastic (FENE) bonds $V^b(r) = -\frac{1}{2}kR_0^2 \ln\left(1 - \frac{r^2}{R_0^2}\right)$, with maximum bond extension $R_0 = 1.5\sigma$ and spring constant $k = 30\epsilon/\sigma^2$.

We integrate the equations of motion using a symplectic Verlet-velocity algorithm in the canonical ensemble with Langevin thermostat [32] using a reduced time-step $\Delta t = 0.005$. Starting from random initial configurations for the monomer and the counterion beads, their equations of motion are evolved for $\sim 10^5$ MD time-steps and thereafter average quantities are computed for another $\sim 10^6$ time-steps. For most of the results (except Fig. 4c,d) the electrode charge density is set to $\Sigma = 0.04$ Cm^{-2} . The effects of polarizability due to dielectric mismatch is taken into account by employing the ICC* (Induced Charge Computation) method [31]; for details of implementation of this algorithm in LAMMPS see Ref. [33]. Briefly, in order to calculate the bound charges due to the dielectric mismatch, we discretize the two interfaces into square grids of area $\sim 0.82\sigma^2$ and use an iterative scheme to obtain the bound charges from the free charges. The computationally expensive calculation of the polarization charges becomes manageable using the ICC* algorithm and yields verifiably accurate results [33].

In order to benchmark the confined polyelectrolyte system, we first run the simulations without surface polarization effect. The time-averaged net charge density profile along the direction of confinement z is defined as $\rho(z) = \rho_+(z) - \rho_-(z)$, where ρ_+ and ρ_- correspond to the charge densities of the positively charged counterions and the negatively charged monomers respectively. In Fig. 2a, $\rho(z)$ is depicted for three different values of the charge fraction f_q . We find that the negatively charged polyelectrolyte chains accu-

mulate near the positive electrode at $z = 0$, whereas the positively charged counterions are seen to accumulate near both the electrodes. This accumulation of counterions near a like-charged electrode is referred to as *charge amplification* (also referred to as *overcharging*) [14, 34, 35] and becomes more pronounced for higher f_q values as can be clearly seen in the inset. This phenomenon arises because the gain in entropy of the counterions is larger than the repulsion it experiences due to the like-charged electrode. However, charge amplification is observed only for low electrode charge densities Σ ; for larger Σ values the repulsion between the electrode and the counterions becomes large and charge amplification disappears. In Fig. 2b we show $\rho(z)$ for an equivalent electrolyte

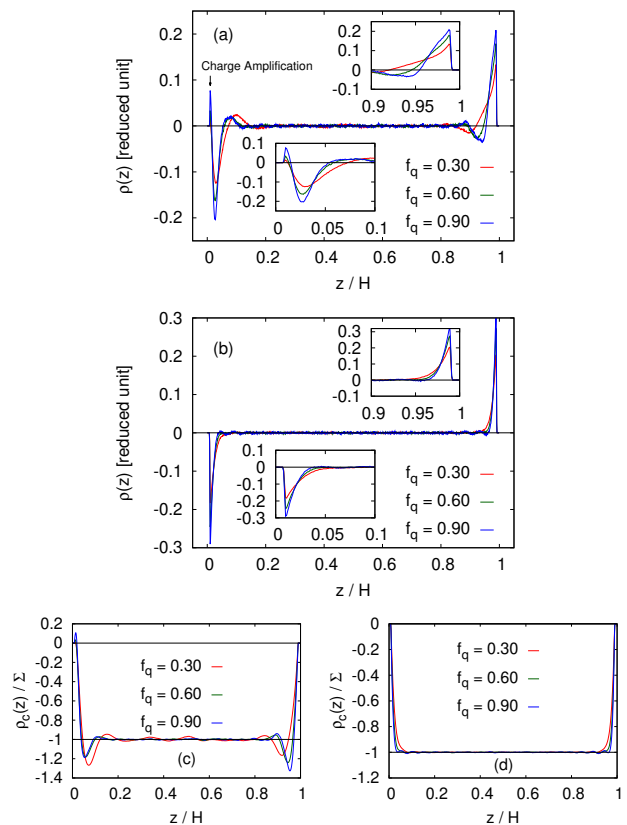


Figure 2. Net charge density profile $\rho(z)$ for different values of the charge fraction f_q for (a) polyelectrolyte solution and (b) electrolyte solution, with all parameters being the same. The insets in both the plots magnify the density profile near the two electrodes. Cumulative charge density $\rho_c(z)$ scaled by the interface charge density Σ for different values of the charge fraction f_q for (c) polyelectrolyte solution and (d) electrolyte solution, computed from the data in (a) and (b) respectively.

solution, which is identical to the polyelectrolyte solution except that all bond potentials are set to zero. The net charge density profile does not show charge amplification and this, as we show below, affects the energy storage of the two systems considerably.

Fig. 2c shows that the cumulative charge density $\rho_c(z) = \int_0^z \rho(s) ds$ for the polyelectrolyte solution near both the elec-

trodes is larger in magnitude than the electrode charge density Σ . This implies that each electrode attracts more charges of the opposite sign than what is necessary to neutralize its charge, which is a phenomenon known as *charge inversion* [35, 36]. Note that, here charge amplification (the positive part of the curve in Fig. 2c) is observed only in the double-layer near the positive electrode but charge inversion is observed near both the electrodes. Thus, the polyelectrolyte solution exhibits charge inversion even if there is no charge amplification, while all these effects are absent in the electrolyte system shown in Fig. 2d.

The effect of surface polarizability on the net charge density profile of the polyelectrolyte solution is shown in Fig. 3a. We find that the density profile of the double-layer is shifted away from the positive electrode (as can be seen in the inset of Fig. 3a); that is, the polyelectrolyte solution experiences more confinement when polarization effects are present. Therefore, the general effect of surface polarizability (when $\epsilon_1 < \epsilon_2$) is to add dielectric confinement on top of the physical confinement due to the impenetrable surfaces at the two ends of the simulation box. There are however subtle differences in how polarization affects different parts of the net charge density profile. A closer look at the two insets in Fig. 3a shows that the peak height of the double-layer formed near the negative electrode decreases in presence of polarization, whereas the peak heights near the positive electrode increase. Thus, in presence of surface polarizability, charge amplification becomes stronger. Although, at the level of the charge density profile, the effect of polarization looks quite small, we show in the following that polarization affects the energy storage and the capacitance of the polyelectrolyte solution significantly.

Interesting features in the conformation of the polyelectrolyte chains are observed in the double-layer formed near the positive electrode. We analyze this by computing the radius of gyration squared $R_g^2 = \frac{1}{N_m} \sum_{i=1}^{N_m} (\vec{r}_i - \vec{r}_{cm})^2$ and its components $R_{g\alpha}^2 = \frac{1}{N_m} \sum_{i=1}^{N_m} (\vec{r}_i^\alpha - \vec{r}_{cm}^\alpha)^2$, where $\alpha \equiv x, y, z$. In Fig. 3b, $3R_{gz}^2(z)/R_g^2$ is shown with and without polarization effects. In the bulk, since $R_{gz}^2 = R_{g\perp}^2 (R_{g\perp}^2 \equiv R_{gx}^2, R_{gy}^2)$, we obtain $3R_{gz}^2(z)/R_g^2 \approx 1$ (since $R_g^2 = R_{gz}^2 + 2R_{g\perp}^2$) and therefore the chains, on an average, have a spherically symmetric conformation. However, next to the left interface $3R_{gz}^2(z)/R_g^2 < 1$, which implies that $R_{gz}^2 < R_{g\perp}^2$. Thus, close to the left electrode, the polyelectrolyte chains are compressed along the z -direction and assume an oblate-spheroid conformation. As one moves towards the bulk from the left electrode, $3R_{gz}^2(z)/R_g^2$ gradually increases and, interestingly enough, at one point it overshoots the bulk value of unity. In this overshoot region, the chains have a prolate-spheroid conformation and are more elongated along the z -direction compared to the perpendicular x, y -directions, that is, $R_{gz}^2 > R_{g\perp}^2$. This z -compressed oblate to a z -elongated prolate conformational change can be explained from the fact that the polyelectrolyte chains near the positive electrode try to minimize the electrostatic repulsion of the neighboring layers of polyelectrolyte chains. Consequently, since the con-

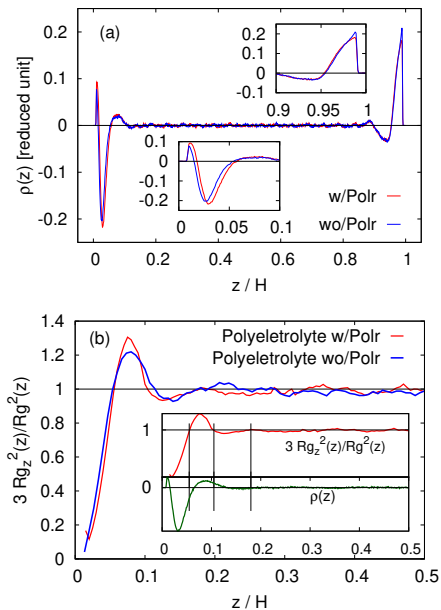


Figure 3. (a) Comparison of the charge density profile $\rho(z)$ of the polyelectrolyte solution for $f_q = 0.90$ with and without polarization effects. (b) The main figure shows $3R_{gz}^2(z)/R_g^2$ for the polyelectrolyte solution with and without polarization for $f_q = 0.40$. In the inset, $3R_{gz}^2(z)/R_g^2$ is shown against the net charge density $\rho(z)$ for the polyelectrolyte solution with polarization effects.

finement effects are stronger in the presence of polarization, this overshooting is more prominent, as seen in Fig. 3b (main figure).

To get a sense of where this *flipping* from z -compressed conformation to a z -elongated conformation happens, we plot $3R_{gz}^2(z)/R_g^2$ along with the net charge density profile $\rho(z)$ of the system in the inset of Fig. 3b. We find that the conformation flipping of the polyelectrolyte chains happens in a region which mostly has a net positive charge (i.e., excess counterions). Also, a closer look at the data in Fig. 3b reveals that this oblate-prolate flipping happens not once but at least twice, before $3R_{gz}^2(z)/R_g^2$ becomes equal to unity in the bulk of the system. Thus, the polyelectrolyte chains near the left interface arrange themselves in alternate layers of z -compressed and z -elongated conformations under confinement. This phenomenon is, in some sense, akin to that of the *cubic* phase observed originally in simulation studies of hard cut spheres [37], although the scenario is much more complicated here.

We measure the electrostatic energy storage in the confined polyelectrolyte solution by first computing the potential profile $\Phi(z)$ between the two electrodes. This is done by numerically integrating the Poisson's equation $\partial_z^2 \Phi(z) = -\rho(z)/(\epsilon_0 \epsilon_r)$, where $\rho(z)$ is the net charge density profile. Typical potential profiles $\Phi(z)$ obtained from the simulations for the polyelectrolyte and the electrolyte solution are shown in Fig. 4a. We denote the potential drop between positive electrode and the bulk as Φ_+ (and similarly for Φ_-) which is

the voltage drop across the electric double-layer (EDL) and referred to as the EDL potential. Note that, for the polyelectrolyte solution $\Phi_+ \neq \Phi_-$, unlike the electrolyte solution. Here, we will focus on the EDL potential Φ_+ since this is the voltage drop across the double-layer formed near the positive electrode where the polyelectrolyte chains get absorbed. The electrostatic energy stored in this EDL (per unit electrode area) is given by $U_+ = \frac{1}{2}\Phi_+Q_+/L^2$, where Q_+ is the total charge in the EDL which is obtained from the simulations. The energy storage U_+ with charge fraction f_q is shown in Fig. 4b. It is found that the energy storage in the polyelectrolyte EDL is higher than the energy stored in the electrolyte EDL. Moreover, we see that energy stored for the polyelectrolyte solution is further enhanced when one takes into account the effects of surface polarizability.

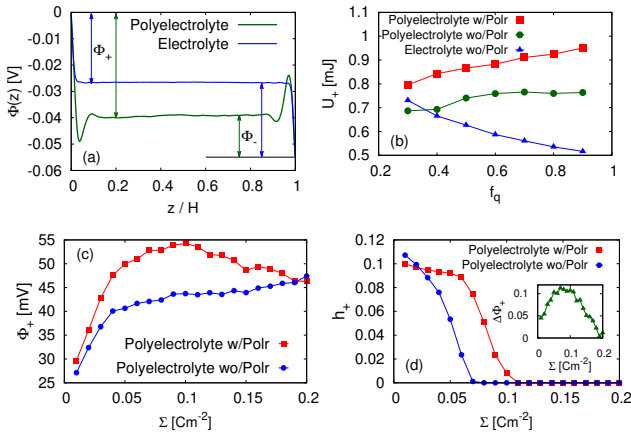


Figure 4. (a) Typical Poisson potential $\Phi(z)$ profiles of polyelectrolyte and electrolyte for charge fraction $f_q = 0.90$. (b) The double-layer energy U_+ with charged fraction f_q for the electrolyte (filled triangles) and polyelectrolyte (filled circles), both without polarization, and polyelectrolyte with polarization (filled squares). The variation of (c) the EDL potential Φ_+ and (d) the height of the charge amplification peak for different values of surface charge density Σ with (filled squares) and without (filled circles) polarization effects. The inset in (d) shows the variation of $\Delta\Phi_+$ (see main text) with surface charge density Σ .

Next, in order to find the differential capacitance C_d , we compute first the double-layer potential Φ_+ for different values of the surface charge density Σ (Fig. 4c). The double-layer potential Φ_+ for the polyelectrolyte in presence of polarization effects is considerably higher than Φ_+ in absence of polarization. Moreover, for the polyelectrolyte *without* polarizability the Φ_+ vs Σ curve is monotonically increasing. (For a monovalent symmetric electrolyte solution without polarization the increase is found to be linear with a roughly constant slope for the same range of Σ values). However, for the polyelectrolyte *with* polarizability effects Φ_+ vs Σ is seen to be non-monotonic. The differential capacitance C_d is defined as the inverse slope of the Φ_+ vs Σ curves, $C_d = (d\Phi_+/d\Sigma)^{-1}$, and thus, it implies that, in presence of polarization effects one obtains a *negative differential capacitance*, $C_d < 0$. As is well

known, equilibrium thermodynamics dictates that the differential capacitance should always be strictly positive because of stability reasons. However, the possibility of a negative differential capacitance under various conditions has been actively investigated (see, for example, [38–40]). Partenskii and coworkers, suggested that the anomalous $C_d < 0$ can emerge in a uniform *charge density controlled* system like ours and this implies that there could be interfacial instabilities and charging induced surface phase transitions in a constant *potential controlled* systems [38]. Such anomalous behavior of the differential capacitance in a uniform surface charge density setup has also been suggested to explain some experimental results [39] recently. Thus, these calculations show that, inclusion of polarization effects not only changes the result in a quantitative way but also significantly changes the qualitative nature of the result.

The disparity in the behavior of the potential Φ_+ in presence and absence of polarizability (Fig. 4c) can be intuitively explained by looking at charge amplification (Fig. 4d). If we denote by h_+ the height of the charge amplification peak (the peak next to the positive electrode in Fig. 2a), we find from Fig. 4d that charge amplification in the polyelectrolyte *without* polarizability effects disappears at $\Sigma = 0.07 \text{ Cm}^{-2}$, whereas the same lingers on till $\Sigma = 0.11 \text{ Cm}^{-2}$ in the presence of polarization effects. This stronger overcharging of the interface leads to a larger value of Φ_+ in the presence of polarization. Thus, although the actual microscopic picture for the emergence of negative differential capacitance seems to be a complicated interplay of charge amplification, electrode charge density Σ , complex changes in polyelectrolyte conformations, etc., one of the reasons seems to be the stronger charge amplification in the presence of surface polarizability effect [23].

Another crucial point to note in Fig. 4c is regarding the importance of polarizability and its dependence on electrode charge density Σ . Although the general belief is that polarizability effects become increasingly unimportant as Σ increases (see [41] and references therein), Fig. 4c demonstrates that this is not true for the electrostatic potential. If we define $\Delta\Phi_+ = \frac{|\Phi'_+ - \Phi_+^0|}{\Phi'_+ + \Phi_+^0}$ as an indicator of the importance of polarization effects, where Φ'_+ and Φ_+^0 are the Φ_+ potential with and without polarizability, we find that $\Delta\Phi_+$ vs Σ has a maximum close to $\Sigma = 0.07 \text{ Cm}^{-2}$, as shown in the inset of Fig. 4d. Thus, the effect of polarizability on the electrostatic potential is found to be most prominent for $\Sigma \approx 0.07 \text{ Cm}^{-2}$ and small on either side of this Σ value.

An intuitive way to understand why there is a large effect of polarizability on the energy storage (Fig. 4b) and differential capacitance (Fig. 4c) but only a nominal effect on the charge density profiles (Fig. 3) is by noting that both energy and differential capacitance depend on the potential Φ , which is a double integral of the charge density profile ρ over the entire confinement, $\Phi(z) \sim \int dz' \int dz'' \rho(z'')$. Thus, the small differences in $\rho(z)$ with and without polarization add up, resulting in large changes in the energy storage and the differential

capacitance.

To summarize, motivated by the design of a supercapacitor, a polyelectrolyte solution confined between two oppositely charged planar dielectric surfaces is studied here via efficient coarse-grained molecular dynamics simulations that include the dielectric discontinuities at the two electrodes. At the level of charge density profiles, the effect due to surface polarization is small. However, surface polarization changes the energy storage and differential capacitance of the confined polyelectrolyte solution significantly. The electrostatic energy stored in the polyelectrolyte double-layer is found to be higher than that of an electrolyte solution, and it is further enhanced when surface polarization effects are taken into account. We also find that the confined polyelectrolyte solution exhibits negative differential capacitance in the presence of surface polarization effects.

Acknowledgement: This work has been funded by NSF DMR Award No. 1611076. We also thank the computational support of Sherman Fairchild Foundation. DB gratefully acknowledges many fruitful discussions with F. J.-Ángeles and A. Ehlen for careful reading of the manuscript.

* E-mail address:debarshee.bagchi@northwestern.edu

† E-mail address:trung.nguyen@northwestern.edu

‡ E-mail address:m-olvera@northwestern.edu

- [1] E. Raspaud, M. Olvera de la Cruz, J.-L. Sikorav, and F. Livolant, *Biophysical Journal* **74**, 381 (1998).
- [2] R. R. Netz and D. Andelman, *Physics Reports* **380**, 1 (2003).
- [3] A. V. Dobrynin and M. Rubinstein, *Progress in Polymer Science* **30**, 1049 (2005).
- [4] S. Buyukdagli, *Physical Review E* **95**, 022502 (2017).
- [5] Y. Levin, *Physica A: Statistical Mechanics and its Applications* **352**, 43 (2005).
- [6] D. Luo and W. M. Saltzman, *Nature Biotechnology* **18**, 33 (2000).
- [7] I. Cakmak, Z. Ulukanli, M. Tuzcu, S. Karabuga, and K. Genc-tav, *European Polymer Journal* **40**, 2373 (2004).
- [8] Y. Huang, M. Zhong, Y. Huang, M. Zhu, Z. Pei, Z. Wang, Q. Xue, X. Xie, and C. Zhi, *Nature Communications* **6**, 10310 (2015).
- [9] A. González, E. Goikolea, J. A. Barrena, and R. Mysyk, *Renewable and Sustainable Energy Reviews* **58**, 1189 (2016).
- [10] M. Vangari, T. Pryor, and L. Jiang, *Journal of Energy Engineering* **139**, 72 (2012).
- [11] P. Simon and Y. Gogotsi, *Nanoscience And Technology: A Collection of Reviews from Nature Journals*, , 320 (2010).
- [12] C. Liu, Z. Yu, D. Neff, A. Zhamu, and B. Z. Jang, *Nano letters* **10**, 4863 (2010).
- [13] H. Yang, S. Kannappan, A. S. Pandian, J.-H. Jang, Y. S. Lee, and W. Lu, *Nanotechnology* **28**, 445401 (2017).
- [14] F. Jiménez-Ángeles and M. Lozada-Cassou, *The Journal of Physical Chemistry B* **108**, 7286 (2004).
- [15] T. Colla, M. Girotto, A. P. dos Santos, and Y. Levin, *The Journal of Chemical Physics* **145**, 094704 (2016).
- [16] A. A. Lee, C. S. Perez-Martinez, A. M. Smith, and S. Perkin, *Physical Review Letters* **119**, 026002 (2017).
- [17] J. W. Zwanikken and M. Olvera de la Cruz, *Proceedings of the National Academy of Sciences* **110**, 5301 (2013).
- [18] H. S. Antila and E. Luijten, *Physical Review Letters* **120**, 135501 (2018).
- [19] H. Li, A. Erbaşlıg, J. Zwanikken, and M. Olvera de la Cruz, *Macromolecules* **49**, 9239 (2016).
- [20] O. A. Hickey and C. Holm, *The Journal of Chemical Physics* **138**, 194905 (2013).
- [21] B. Qiao, J. J. Cerda, and C. Holm, *Macromolecules* **44**, 1707 (2011).
- [22] Y. Jing, V. Jadhao, J. W. Zwanikken, and M. Olvera de la Cruz, *The Journal of Chemical Physics* **143**, 194508 (2015).
- [23] G. I. Guerrero García and M. Olvera de la Cruz, *The Journal of Physical Chemistry B* **118**, 8854 (2014).
- [24] M. Girotto, R. M. Malossi, A. P. dos Santos, and Y. Levin, *The Journal of Chemical Physics* **148**, 193829 (2018).
- [25] A. P. dos Santos, M. Girotto, and Y. Levin, *The Journal of Chemical Physics* **144**, 144103 (2016).
- [26] A. P. dos Santos, M. Girotto, and Y. Levin, *The Journal of Physical Chemistry B* **120**, 10387 (2016).
- [27] A. P. dos Santos and Y. Levin, *The Journal of Chemical Physics* **142**, 194104 (2015).
- [28] R. Messina, *Physical Review E* **70**, 051802 (2004).
- [29] R. Messina, *Physical Review E* **74**, 049906 (2006).
- [30] M. J. Stevens and K. Kremer, *Physical Review Letters* **71**, 2228 (1993).
- [31] S. Tyagi, M. Süzen, M. Sega, M. Barbosa, S. S. Kantorovich, and C. Holm, *The Journal of Chemical Physics* **132**, 154112 (2010).
- [32] D. Frenkel and B. Smit, *Understanding molecular simulation: from algorithms to applications*, Vol. 1 (Elsevier, 2001).
- [33] T. D. Nguyen, H. Li, D. Bagchi, F. J. Solis, and M. Olvera de la Cruz, *Computer Physics Communications* (2019).
- [34] G. I. Guerrero-García, E. González-Tovar, M. Chávez-Páez, and M. Lozada-Cassou, *The Journal of Chemical Physics* **132**, 054903 (2010).
- [35] G. I. Guerrero-García, E. González-Tovar, and M. Olvera de la Cruz, *Soft Matter* **6**, 2056 (2010).
- [36] R. Messina, E. González-Tovar, M. Lozada-Cassou, and C. Holm, *EPL (Europhysics Letters)* **60**, 383 (2002).
- [37] J. Veerman and D. Frenkel, *Physical Review A* **45**, 5632 (1992).
- [38] M. B. Partenskii, V. Dorman, and P. C. Jordan, *International Reviews in Physical Chemistry* **15**, 153 (1996).
- [39] M. B. Partenskii and P. C. Jordan, *Physical Review E* **77**, 061117 (2008).
- [40] M. B. Partenskii and P. C. Jordan, *Physical Review E* **80**, 011112 (2009).
- [41] M. M. Hatlo and L. Lue, *Soft Matter* **4**, 1582 (2008).